Bioorganic Chemistry 84 (2019) 170–176

Contents lists available at ScienceDirect

Bioorganic Chemistry

journal homepage: www.elsevier.com/locate/bioorg

1-(2-Hydroxy-5-((trimethylsilyl)ethynyl)phenyl)ethanone based α,β-unsaturated derivatives an alternate to non-sulfonamide carbonic anhydrase II inhibitors, synthesis via Sonogashira coupling, binding analysis, Lipinsk's rule validation

Jamaluddin Mahar[a,b], Aamer Saeed[a,*], Kevin D. Belfield[b], Fayaz Ali Larik[a,*], Pervaiz Ali Channar[a], Mehar Ali Kazi[c], Qamar Abbas[d], Mubashir Hassan[e], Hussain Raza[e], Sung-Yum Seo[e]

[a] Department of Chemistry, Quaid-I-Azam University, Islamabad 45320, Pakistan
[b] Department of Chemistry, School of Optics/Center for Research and Education in Optics and Lasers University of Central Florida, P.O. Box 162366, Orlando, FL 32816, United States
[c] Institute of Biochemistry, University of Sindh, Jamshoro 76080, Pakistan
[d] Department of Physiology, University of Sindh, Jamshoro 76080, Pakistan
[e] Department of Biological Sciences, College of Natural Sciences, Kongju National University, 56 Gongjudehak-Ro, Gongju, Chungnam 314-701, Republic of Korea

ARTICLE INFO

Keywords:
Sonogashira coupling
Claisen-Schmidt reaction
Silyl yne chalcone derivtaives
Carbonic anhydrase-II
Binding analysis
Lipinsk's rule

ABSTRACT

A novel series of silyl-yne containing chalcone derivatives **5a-5j** was synthesized by exploiting Sonogashira coupling reaction and Claisen-Schimdt condensation reaction. The synthesized derivative were characterized by spectroscopic and elemental analysis. The selective inhibition of carbonic anhydrases is considered critical in the field of medicinal chemistry because carbonic anhydrases exits in several isoforms. Synthesized compounds were subjected to carbonic anhydrase –II assay. Except **5j**, the other derivatives exhibited better potential than standard acetazolamide. Compound **5e** was found to be potent derivative in the series with IC_{50} value 0.054 ± 0.001 μM. Binding analysis revealed that most potent derivative 5e binds in the active site of CA-II and single π-π stacking interaction was observed between ring structure of ligand and Phe129 having bond length 4.90 Å. Pharmacokinetics elicited that compounds obey Lipinski's rule and show significant drug score.

1. Introduction

The carbonic anhydrases (CAs, EC 4.2.1.1) are widely distributed among prokaryotes and eukaryotes. These are zinc containing metalloenzymes and are divided into distinct three gene families. α-CAs (present in vertebrates, eubacteria, algae and cytoplasm of green plants), the β-CAs (predominantly in eubacteria, algae and chloroplasts of both mono- as well as dicotyledons) and the γ-CAs (mainly in Archaea and some eubacteria), respectively. In higher vertebrates, carbonic anhydrases exists in various different isoforms, particularly α-class CAs are very relevant clinical family with 14 known isoforms found in mammalian tissues [1–5]. Carbonic II anhydrase is the first member of zinc depended α-CAs which was thoroughly characterized in 1933. CA-II is a subcellular cystol bound enzyme and elicits high CO_2 catalytic activity. CA-II is involved in the catalysis of reaction between carbon dioxide and bicarbonate ion and thus play critical role in physiological processes such as respiration and movement of carbon dioxide/bicarbonate, homeostasis balance of CO_2 and pH, biosynthetic reactions (such as gluconeogenesis, lipogenesis and ureagenesis), bone resorption, calcification and tumorigenicity [6–8]. Up until now, the carbonic anhydrase II inhibitors are based on sulfonamides, sulfamate and hydroxysulfamates [9–12]. However, sulfonamides have dominated the drug industry for the designing of therapeutic agents for the inhibition of carbonic anhydrase II. Treatment of glaucoma requires high doses of sulfonamide drugs and this sometimes results in some side effects such as altered taste, malaise, fatigue, depression, and anorexia. Allergic adverse effect has been observed in some human being who intake sulfonamide based drugs. Thus we envisioned to seek potential small organic compounds based on non-sulfonamide moiety and evaluate their role as inhibitors of carbonic anhydrase II enzyme.

* Corresponding authors.
E-mail addresses: aamersaeed@yahoo.com (A. Saeed), fayazali@chem.qau.edu.pk (F. Ali Larik).

https://doi.org/10.1016/j.bioorg.2018.11.031
Received 13 May 2018; Received in revised form 12 November 2018; Accepted 20 November 2018
Available online 24 November 2018
0045-2068/

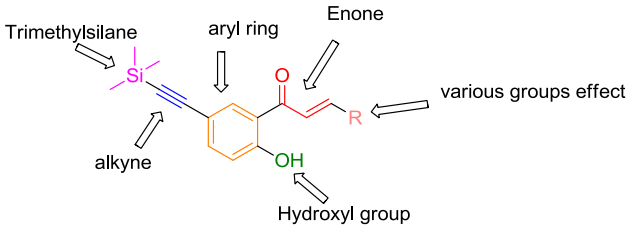

Fig. 1. Structural features linked with synthesized molecule.

α,β-unsaturated derivatives of carbonyl compounds are known as Chalcones. Chalcone derivatives can be synthesized by using Claisen-Schmidt condensation reaction. Chalcone derivatives serve as valuable synthon for the synthesis of wide variety of heterocycles. The enone moiety in chalones play the crucial role in the synthesis of chalone derivatives. Chalcones and their derivatives, whether synthetic or naturally occurring are an interesting and significant group of molecules as they possess a wide range of pharmacological activities such as anti-inflammatory, antimicrobial, antifungal, antibacterial, antioxidant, cytotoxic, anti-tumor, anticancer, antimitotic, antileishmanial, antimalarial, antitubercular, and antiviral [13–18].

A number of chalcone derivatives are reported to inhibit enzymes such as xanthine oxidase, aldose reductase, epoxide hydrolase, protein tyrosine kinase, quinone reductase, monoamine oxidase and lipoxygenase [19,20]. Herein, we have designed the chalcone derivatives (Fig. 1) to explore their potential as inhibitors of carbonic anhydrase- II enzyme.

2. Experimental

2.1. Materials and methods

Fluorene, 4-iodophenol, acetyl chloride, trimethylamine, ethynyltrimethylsilane, copper(I)iodide, bis(triphenylphosphine)palladium(II) dichloride, 4-(dimethylamino)benzaldehyde, 1-hydroxy-2-naphthaldehyde. Reactions were carried out under a N_2 atmosphere. THF was freshly distilled from Na and benzophenone ketyl. $AlCl_3$ was purified by sublimation before use. All other reagents and solvents were used as received from commercial suppliers. ^1H and ^{13}C NMR spectra were recorded on an NMR spectrometer at 300 and 75 MHz, respectively.

2.2. General procedure for the synthesis of 1-(2-hydroxy-5 ((trimethylsilyl) ethynyl)phenyl) ethanone based α,β-unsaturated derivatives

Synthesis of 1-(2-Hydroxy-5-((trimethylsilyl)ethynyl)phenyl)ethanone based α,β-unsaturated derivatives were achieved by using 1-(2-hydroxy-5-((trimethylsilyl)ethynyl)phenyl)ethanone and aromatic aldehydes in equivalent ratio, using piperidine (1.5 eq) as catalyst, in ethanol. Reaction mixture was refluxed for 15 h until the reaction was completed, then reaction was cooled to room temperature. Mixture was diluted with distilled water and neutralized with dilute HCl, precipitated product was filtered and recrystallized from ethanol.

2.3. Experimental data

2.3.1. 1-(2-Hydroxy-5-((trimethylsilyl)ethynyl)phenyl)-3-phenylprop-2-en-1-one (5a)

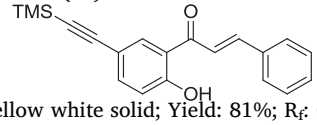

Yellow white solid; Yield: 81%; R_f: 0.69; m.p. 169–171 °C; FTIR (Neat, cm^{-1}) υ_{max}: 3380 (O-H), 3063 (C=C-H), 2928 (C-H_{str}), 2852 (C-H_{str}), 1694 (Ar-C=O), 1603 (C=C αβ-unsaturated), 1597(Aromatic, C=C_{str}); 837 (Si-H); ^1H NMR (300 MHz, $CDCl_3$) δ 8.29 (s, 1H), 8.22 (d, J = 15.0 Hz, 1H), 7.87 (d, J = 15 Hz, 1H), 7.76–7.43 (m, 6H), 6.91 (d, J = 7.5 Hz, 1H), 4.32 (s, 1H), 0.35 (s, 9H); ^{13}C NMR (75 MHz, $CDCl_3$) δ 192.5, 161.1, 143.9, 137.0, 135.9, 134.2, 129.5, 129.0, 128.1, 125.2, 122.2, 120.6, 115.6, 106.7, 104.2, 0.2; MS (*m/z*, APCI): calcd 320.46 (M^+), found 322.41 [M + 2H]

2.3.2. 3-(4-(dimethylamino)phenyl)-1-(2-hydroxy-5-((trimethylsilyl) ethynyl)phenyl)prop-2-en-1-one (5b)

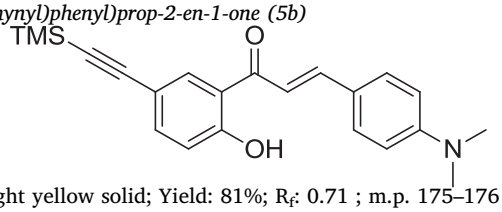

Light yellow solid; Yield: 81%; R_f: 0.71 ; m.p. 175–176 °C; FTIR (Neat, cm^{-1}) υ_{max}: 3382 (O-H), 3061 (C=C-H), 2930 (C-H_{str}), 2848 (C-H_{str}), 1700 (Ar-C=O), 1601 (C=C αβ-unsaturated), 1596(Aromatic, C=C_{str}); 1370 (–CH_3), 1276 (C-N), 839 (Si-C); ^1H NMR (300 MHz, $CDCl_3$) δ 8.25 (s, 1H), 8.19 (d, J = 15.0 Hz, 1H), 7.86 (d, J = 15 Hz, 1H), 7.57 (d, J = 7.5, Hz, 1H), 7.37 (d, J = 7.5, Hz, 1H), 6.90 (d, J = 7.5 Hz, 2H), 6.78 (d, J = 7.5 Hz, 2H), 3.99 (s, 1H), 2.93 (s, 6H), 0.23 (s, 9H); ^{13}C NMR (75 MHz, $CDCl_3$) δ 192.5, 161.1, 151.1, 143.9, 137.0, 134.2, 129.9, 125.2, 123.8, 122.2, 120.6, 115.3, 112.7, 106.7, 104.2, 41.9, 0.2; MS (*m/z*, APCI): calcd 363.25 (M^+), found 365.25 [M + 2H]

2.3.3. 1-(2-Hydroxy-5-((trimethylsilyl)ethynyl)phenyl)-3-(pyridin-3-yl) prop-2-en-1-one (5c)

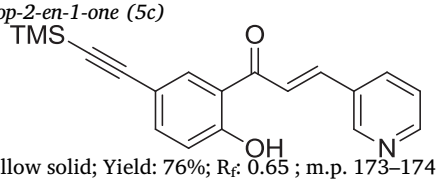

Yellow solid; Yield: 76%; R_f: 0.65 ; m.p. 173–174 °C; FTIR (Neat, cm^{-1}) υ_{max}: 3352 (O-H), 3090 (C=C-H), 2926 (C-H_{str}), 2836 (C-H_{str}), 1701 (Ar-C=O), 1629 (C=N), 1600 (C=C αβ-unsaturated), 1590(Aromatic, C=C_{str}); 1273 (C-N), 840 (Si-C);^1H NMR (300 MHz, $CDCl_3$) δ 8.68 (s, 1H), 8.61 (d, J = 7.5 Hz, 1H), 8.15 (d, J = 15.0 Hz, 1H), 7.92 (d, J = 15.0 Hz, 1H), 7.83 (s, 1H), 7.78 (d, J = 7.5 Hz, 1H), 7.51 (t, J = 7.5 Hz, 1H), 7.37 (d, J = 7.5 Hz, 1H), 6.92 (d, J = 7.5 Hz, 1H), 4.19 (s, 1H), 0.30 (s, 9H); ^{13}C NMR (75 MHz, $CDCl_3$) δ 192.5, 161.1, 149.7, 149.1, 139.9, 137.0, 135.8, 134.2, 131.2, 125.2, 123.4, 122.3, 120.6, 115.6, 106.7, 104.2, 0.15; MS (*m/z*, APCI): calcd 321.45 (M^+), found 323.39 [M + 2H]

2.3.4. 1-(2-Hydroxy-5-((trimethylsilyl)ethynyl)phenyl)-3-(4-methoxyphenyl)prop-2-en-1-one (5d)

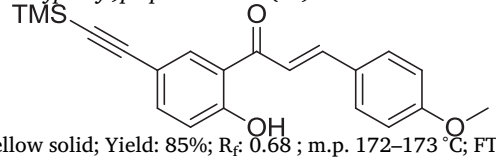

Yellow solid; Yield: 85%; R_f: 0.68 ; m.p. 172–173 °C; FTIR (Neat, cm^{-1}) υ_{max}: 3348 (O-H), 3092 (C=C-H), 2927 (C-H_{str}), 2838 (C-H_{str}), 1698 (Ar-C=O), 1627 (C=N), 1599 (C=C αβ-unsaturated), 1588 (Aromatic, C=C_{str}); 1212 (C-O), 837 (Si-C); ^1H NMR (300 MHz, $CDCl_3$) δ 8.19 (s, 1H), 7.95 (d, J = 15 Hz, 1H), 7.86 (d, J = 7.5 Hz, 1H), 7.69 (d, J = 7.5 Hz, 2H), 7.59 (d, J = 7.5 Hz, 1H), 7.32 (d, J = 15 Hz, 1H), 7.04 (d, J = 7.5 Hz, 2H), 3.95 (s, 1H), 3.81 (s, 3H), 0.35 (s, 9H); ^{13}C NMR (75 MHz, $CDCl_3$) δ 192.5, 161.1, 160.8, 143.9, 137.0, 134.2, 129.4, 128.7, 125.2, 122.2, 120.6, 115.6, 114.6, 106.7, 104.2, 56.0, 0.15; MS (*m/z*, APCI): calcd 340.48 (M^+), found 343.48 [M + 3H]

2.3.5. 1-(2-hydroxy-5-((trimethylsilyl)ethynyl)phenyl)-3-(4-(phenoxymethyl)phenyl)prop-2-en-1-one (5e)

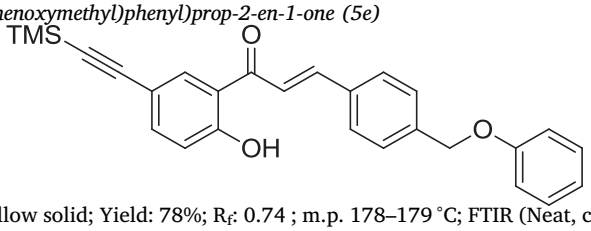

Yellow solid; Yield: 78%; R_f: 0.74 ; m.p. 178–179 °C; FTIR (Neat, cm^{-1}) υ_{max}: 3369 (O-H), 3080 (C=C-H), 2928 (C-H_{str}), 1703 (Ar-C=O), 1602 (C=C αβ-unsaturated), 1598(Aromatic, C=C_{str}); 1465 (–CH_2), 1215 (C-O), 840 (Si-C);^{1}H NMR (300 MHz, $CDCl_3$) δ 8.55 (s, 1H), 8.34 (d, J = 15 Hz, 1H), 7.95 (d, J = 8.3 Hz, 1H), 7.61 (d, J = 7.5 Hz, 2H), 7.49 (d, J = 15 Hz, 1H), 7.40 (d, J = 8.1 Hz, 2H), 7.36 (d, J = 7.5 Hz, 2H), 7.30 (d, J = 8.3 Hz, 1H), 7.24 (t, J = 7.5 Hz, 1H), 6.97 (d, J = 7.5 Hz, 2H), 5.16 (s, 2H), 0.38 (s, 9H); ^{13}C NMR (75 MHz, $CDCl_3$) δ 192.5, 161.1, 159.2, 143.9, 137.0, 135.0, 134.2, 129.5, 128.1, 127.1, 125.2, 122.2, 121.5, 120.6, 115.7, 115.6, 106.7, 104.2, 70.8, 0.2; MS (*m/z*, APCI): calcd 426.58 (M^+), found 428.56 [M + 2H]

2.3.6. 1-(2-hydroxy-5-((trimethylsilyl)ethynyl)phenyl)-3-(4-((4-methoxyphenoxy)methyl)phenyl)prop-2-en-1-one (5f)

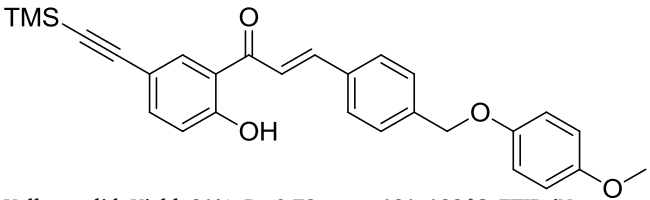

Yellow solid; Yield: 81%; R_f: 0.73 ; m.p. 181–182 °C; FTIR (Neat, cm^{-1}) υ_{max}: 3363(O-H), 3078 (C=C-H), 2930 (C-H_{str}), 1702 (Ar-C=O), 1600 (C=C αβ-unsaturated), 1590(Aromatic, C=C_{str}); 1465 (–CH_2), 1378 (–CH3), 1213 (C-O), 835 (Si-C);^{1}H NMR (300 MHz, $CDCl_3$) δ 8.80 (s, 1H), 8.12 (d, J = 15.0 Hz, 1H), 8.67 (d, J = 7.3 Hz, 1H), 8.64 (d, J = 7.5 Hz, 2H), 7.58 (d, J = 15.0 Hz, 1H), 7.38 (d, J = 7.5 Hz, 2H), 7.13 (d, J = 7.3 Hz, 1H), 6.95 (s, 4H), 5.18 (s, 2H), 3.82 (s, 3H), 0.08 (s, 9H); ^{13}C NMR (75 MHz, $CDCl_3$) δ 192.5, 161.1, 154.7, 154.2, 143.9, 137.0, 137.0, 135.0, 134.2, 128.1, 127.1, 125.2, 122.2, 120.6, 117.1, 115.6, 115.1, 106.7, 104.2, 70.8, 56.0, 0.2; MS (*m/z*, APCI): calcd 456.61 (M^+), found 459.47 [M + 3H]

2.3.7. 1-(2-hydroxy-5-((trimethylsilyl)ethynyl)phenyl)-3-(pyren-1-yl) prop-2-en-1-one (5 g)

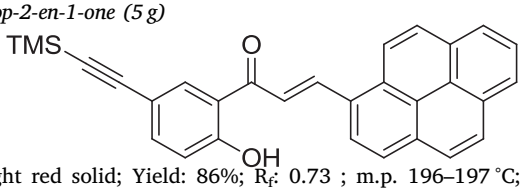

Light red solid; Yield: 86%; R_f: 0.73 ; m.p. 196–197 °C; FTIR (Neat, cm^{-1}) υ_{max}: 3352 (O-H), 3065 (C=C-H), 2930 (C-H_{str}), 1702 (Ar-C=O), 1607 (C=C αβ-unsaturated), 1598(Aromatic, C=C_{str}); 834 (Si-C);^{1}H NMR (300 MHz, $CDCl_3$) δ 8.73 (s, 1H), 8.67 (d, J = 7.3 Hz, 1H), 8.61 (d, J = 7.5 Hz, 2H), 8.10 (d, J = 15.0 Hz, 1H), 8.06–7.79 (m, 5H),7.71 (s, 1H), 7.54 (d, J = 15.0 Hz, 1H), 7.35 (d, J = 7.5 Hz, 2H), 7.09 (d, J = 7.3 Hz, 1H)

3.80 (s, 1H), 0.33 (s, 9H); ^{13}C NMR (75 MHz, $CDCl_3$) δ 192.5, 161.1, 138.0, 137.0, 134.2, 134.2, 131.6, 131.4, 129.5, 128.7, 128.3, 128.2, 128.2, 128.0, 127.8, 127.4, 125.2, 125.2, 124.9, 124.0, 123.6, 120.6, 115.6, 106.7, 104.2, 0.2; MS (*m/z*, APCI): calcd 444.60 (M^+), found 445.59 [M + H]

2.3.8. 1-(4-(4-(3-(2-hydroxy-5-((trimethylsilyl)ethynyl)phenyl)-3-oxoprop-1-en-1-yl)-2,6-dimethoxyphenoxy)butyl)pyrrolidine-2,5-dione (5 h)

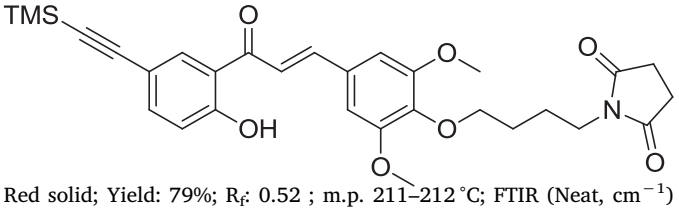

Red solid; Yield: 79%; R_f: 0.52 ; m.p. 211–212 °C; FTIR (Neat, cm^{-1}) υ_{max}: 3328 (O-H), 3073 (C=C-H), 2928 (C-H_{str}), 1702 (Ar-C=O), 1685 (C=O amide), 1605 (C=C αβ-unsaturated), 1596 (Aromatic, C=C_{str}); 1373 (C-N), 841 (Si-C);^{1}H NMR (300 MHz, $CDCl_3$) δ 7.98 (d, J = 15.0 Hz, 1H), 7.84 (d, J = 1.4 Hz, 1H), 7.57 (dd, J = 7.5, 1.4 Hz, 1H), 7.39 (d, J = 15.0 Hz, 1H), 6.93–6.87 (m, 3H), 4.09 (t, J = 7.6 Hz, 2H), 3.96 (s, 1H), 3.83 (s, 6H), 3.56 (t, J = 7.6 Hz, 2H), 2.87 (s, 4H), 1.74 (dq, J = 7.6, 5.6 Hz, 2H), 1.58 (tt, J = 7.5, 5.6 Hz, 2H), 0.35 (s, 9H); ^{13}C NMR (75 MHz, $CDCl_3$) δ 192.5, 178.2, 161.1, 153.1, 143.5, 140.9, 137.0, 134.2, 130.9, 125.2, 122.9, 120.6, 115.6, 106.7, 105.8, 104.2, 72.7, 56.8, 36.3, 28.4, 27.5, 26.8, 0.2; MS (*m/z*, APCI): calcd 549.69 (M^+), found 555.69 [M + 6H]

2.3.9. 3-(4-(diethylamino)phenyl)-1-(2-hydroxy-5-((trimethylsilyl) ethynyl)phenyl)prop-2-en-1-one (5i)

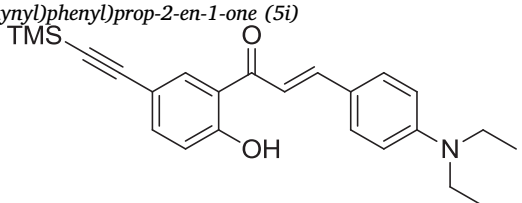

Yellow solid; Yield: 83%; R_f: 0.70 ; m.p. 178–179 °C; FTIR (Neat, cm^{-1}) υ_{max}: 3333 (O-H), 3078 (C=C-H), 2928 (C-H_{str}), 1702 (Ar-C=O), 1685 (C=O amide), 1608 (C=C αβ-unsaturated), 1592 (Aromatic, C=C_{str}); 1460 (–CH_2), 1368 (–CH_3), 1278 (C-N), 836 (Si-C);^{1}H NMR (300 MHz, $CDCl_3$) δ 8.18 (d, J = 15.0 Hz, 1H), 7.85 (d, J = 1.4 Hz, 1H), 7.76 (d, J = 7.5 Hz, 2H), 7.72 (dd, J = 7.5, 1.4 Hz, 1H), 7.42 (d, J = 15 Hz , 1H), 6.90 (d, J = 7.5 Hz, 1H), 6.80 (d, J = 7.5 Hz, 2H), 3.96 (s, 1H), 3.61 (q, J = 6.3 Hz, 4H), 1.21 (t, J = 6.3 Hz, 6H), 0.23 (s, 9H); ^{13}C NMR (75 MHz, $CDCl_3$) δ 192.5, 161.1, 148.8, 143.9, 137.0, 134.2, 131.9, 125.2, 123.0, 122.2, 120.6, 115.6, 110.5, 106.71104.2, 46.3, 13.0, 0.2; MS (*m/z*, APCI): calcd 391.58 (M^+), found 393.57 [M + 2H]

2.3.10. 1-(2-Hydroxy-5-((trimethylsilyl)ethynyl)phenyl)-3-(pyridin-4-yl) prop-2-en-1-one (5j)

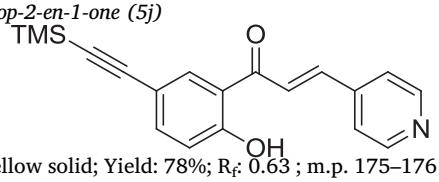

Yellow solid; Yield: 78%; R_f: 0.63 ; m.p. 175–176 °C; FTIR (Neat, cm^{-1}) υ_{max}: 3350 (O-H), 3092 (C=C-H), 2928 (C-H_{str}), 1705 (Ar-C=O), 1630 (C=N), 1600 (C=C αβ-unsaturated), 1590(Aromatic, C=C_{str}); 1267 (C-N), 835 (Si-C);^{1}H NMR (300 MHz, $CDCl_3$) δ 8.59 (d, J = 7.4 Hz, 2H), 8.19 (d, J = 15.0 Hz, 1H), 8.04 (s, 1H), 7.90 (d, J = 15.0 Hz, 1H), 7.58 (d, J = 7.5 Hz, 1H), 7.37 (d, J = 7.4 Hz, 2H), 6.91 (d, J = 7.5 Hz, 1H), 4.34 (s, 1H), 0.34 (s, 9H); ^{13}C NMR (75 MHz, $CDCl_3$) δ 192.5, 161.1, 151.5, 143.9, 143.2, 137.0, 134.2, 125.2, 122.2, 121.7, 120.6, 115.6, 106.7, 104.2, 0.2; MS (*m/z*, APCI): calcd 321.45(M^+), found 323.09 [M + 2H]

2.4. Carbonic anhydrase assay

Carbonic anhydrase inhibition was measured as described previously with some modifications [21]. The method is based on the principle that *p*-nitrophenyl acetate is hydrolyzed by Carbonic anhydrase to form yellow colored *p*-nitrophenol which was measured spectrophotometrically. Briefly, Reaction mixture contained 120 µL of 50 mM Tris-sulfate buffer (pH 7.6 containing 0.1 mM $ZnCl_2$), 20 µL of

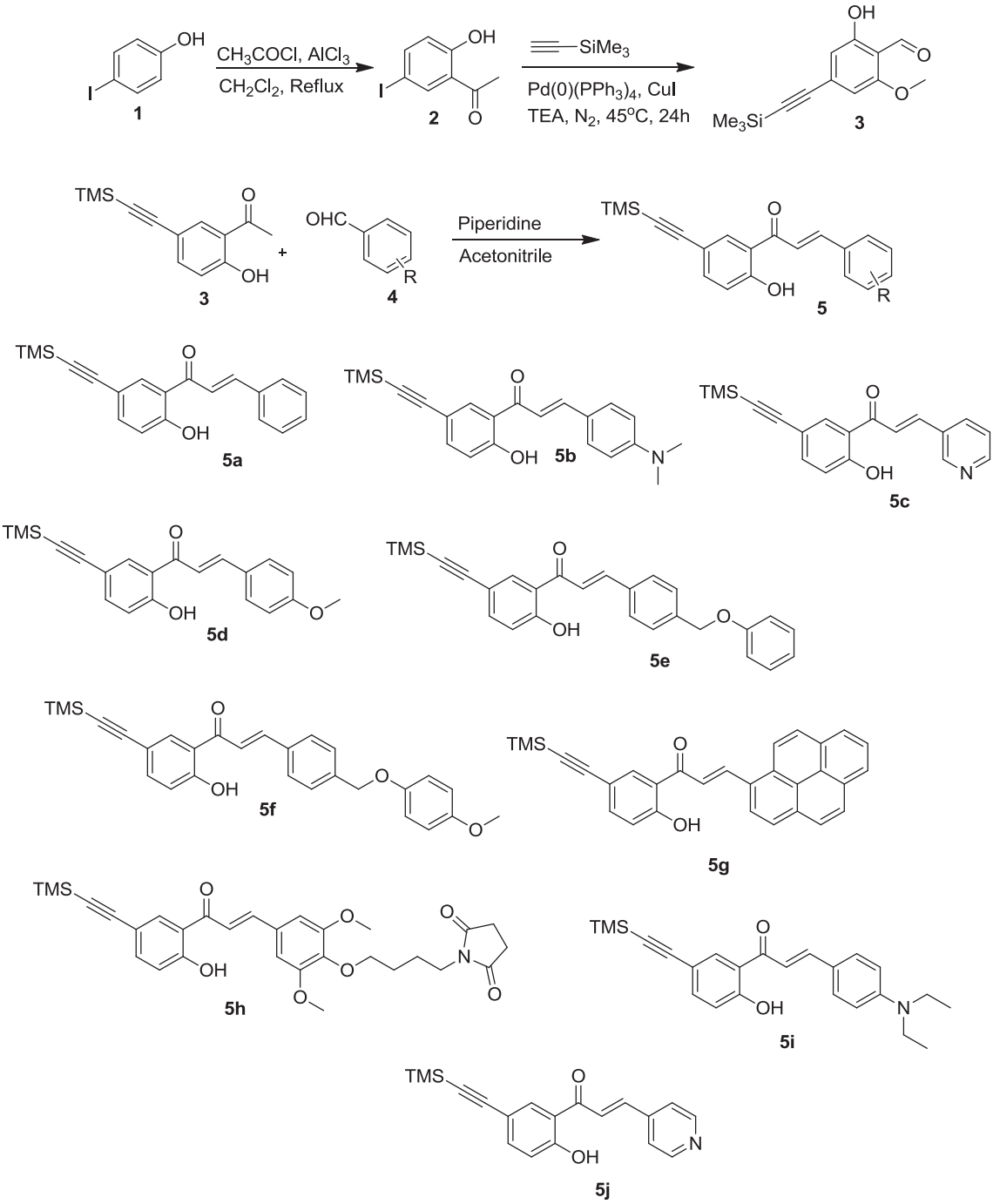

Scheme 1.

inhibitor and 20 μL (50 U) bovine enzyme per well. Contents were well mixed and pre-incubated at 25 °C for 10 min. substrate *p*-nitrophenyl acetate was prepared (6 mM stock using < 5% acetonitrile in buffer and used fresh every time) and 40 μL was added per well to achieve 0.6 mM concentration per well. Total reaction volume was made to 200 μL. After30 min incubation at 25 °C contents were mixed and absorbance was measured at 348 nm using a microplate reader. Acetazolamide was used as a reference inhibitor and tris-sulfate buffer was used as negative control. Each concentration was analyzed in three independent experiments. IC_{50} values were calculated by nonlinear regression using GraphPad Prism 5.0.

$$\text{Inhibition}(\%) = [(B - S)/B] \times 100$$

Here, the B and S are the absorbances for the blank and samples.

2.5. Free radical scavenging assay

Radical scavenging activity was determined by modifying method by 2, 2-diphenyl-1-picrylhydrazyl (DPPH) assay [22]. The assay solution consisted of 100 mL of (150 mM) 2,2-diphenyl-1 picrylhydrazyl (DPPH), 20 μL of increasing concentration of test compounds and the volume was adjusted to 200 μL in each well. This reaction mixture was then incubated for 30 min at room temperature. Ascorbic acid (Vitamin C) was used as a reference inhibitor. The measurements were carried out by using a micro plate reader (OPTIMax, tunable) at 517 nm. The reaction rates were compared and the percent inhibition due to the presence of tested inhibitors was calculated. Each concentration was analyzed in three independent experiments.

2.6. Selection of carbonic anhydrase II from PDB

The crystal structure of carbonic anhydrase II was retrieved form the Protein Data Bank (PDB) having PDBID 1V9E (www.rcsb.org). Energy minimization of target structure was carried out by using conjugate gradient algorithm and Amber force field in UCSF Chimera 1.10.1. The stereo-chemical properties, Ramachandran graph and values of Carbonic anhydrase II structure were assessed by Molprobity server, while the hydrophobicity graph was generated by Discovery Studio 4.1 Client. The protein architecture and statistical percentage values of helices, beta-sheets, coils and turns were accessed by using online tool VADAR 1.8.

3. *In-silico* designing of synthesized ligands and Lipinski rule validation

The synthesized ligand molecules (5a-5j) were sketched in drawing ACD/ChemSketch tool and further minimized by visualizing software UCSF Chimera 1.10.1. The different online drug assessment tools like Molinspiration (http://www.molinspiration.com/) and Molsoft (http://www.molsoft.com/) were employed to predict the drug-likeness and biological properties of these designed candidate molecules. The number of rotatable bonds, hydrogen bond acceptors (HBA) and hydrogen bond donors (HBD) were also confirmed by PubChem (https://pubchem.ncbi.nlm.nih.gov/). Moreover, Lipinski's rule of five was analyzed using Molsoft and Molinspiraion tools.

3.1. Molecular docking

The docking experiment against target protein and ligands was performed using PyRx docking tool [23]. The grid box center values of (center_X = 11.6361, center_Y = 47.8016 and center_ Z = 22.1317) and size values were adjusted as (X = 46.4690, Y = 50.6562, and Z = 50.9719) for better conformational position in the active region of target protein. The synthesized ligands (5a-5j) were docked separately against carbonic anhydrase II with default exhaustiveness value = 8. The predicted docked complexes were evaluated on the basis of lowest binding energy (Kcal/mol) values and structure activity relationship (SAR) analyses. The three dimensional (3D) graphical depictions of docked complexes were accomplished by Discovery Studio (2.1.0) and UCSF Chimera 1.10.1 tool. The two dimensional graphical depictions of other complexes was generated by LIGPLOT [24].

4. Results and discussions

4.1. Chemistry

The synthesis of silyl group containing chalcone derivatives has been outlined in Scheme 1. 4-Iodophenol **1** was used starting precursor. **1** was reacted under Friedel Crafts reaction conditions to obtained acylated product **2.** Ethenyl silyl group was reacted using Sonogashira coupling protocol to afforded silylated product **3**. In the last step various substituted aromatic aldehydes were reacted with 3 to obtain the desired product (5a-5j) in good yield and high purity.

4.2. Carbonic anhydrase II inhibitory activity

Table 1 displays the results of carbonic anhydrase II inhibition assay in micromolar range. The IC_{50} values of the compounds **5a-5j** reveal that except **5j,** other derivatives showed better potential than the reference acetazolamide (IC_{50} 0.998 ± 0.024 μM). Various substituents were attached with chalcone linkage. Compounds **5c** and **5j** bear pyridine rings. In case of compound **5c** the results of CA-II inhibition are better than **5j**. Compounds **5b** and **5i** possess *N*,*N*-dimethyl and *N*,*N*-diethyl groups and compound **5b** expressed significant potential than **5i**. Ether linkages were also imparted in the chalcone derivatives such as **5d, 5e** and **5f**. Compound **5d** contains methoxy group at para position of phenyl ring and exhibited higher inhibition potency compared to **5f**. Derivative 6e also possessed ether moiety and showed better activity compared to **5d** and **5e**. Compound **5g** contains perylene entity and it showed better activity compared to standard acetazolamide. Molecule **5h** contained multifunctional groups and showed good CA-II inhibition.

Table 1
Carbonic anhydrase II activity and radical scavenging activity of chalcone derivatives (5a-5j).

Compound	Carbonic anhydrase (IC_{50} μM)	Radical Scavenging %	Energy Values (Kcal/mol)
5a	0.356 ± 0.008	39.708 ± 1.538	−7.1
5b	0.093 ± 0.002	75.786 ± 1.96	−7.3
5c	0.033 ± 0.008	55.966 ± 2.16	−7.7
5d	0.205 ± 0.004	43.035 ± 1.66	−6.9
5e	0.054 ± 0.001	94.312 ± 3.65	−7.7
5f	0.577 ± 0.013	97.251 ± 3.766	−7.5
5g	0.093 ± 0.002	10.731 ± 0.14	−8.7
5h	0.992 ± 0.024	59.422 ± 2.3	−8.4
5i	0.131 ± 0.003	35.998 ± 1.29	−7.3
5j	0.910 ± 0.022	52.157 ± 2.02	−6.9
Acetazolamide	0.998 ± 0.024	–	–
Vitamin C	–	96.422 ± 3.35	–

For calculation of IC_{50} six to eight concentrations were used. IC_{50} values were calculated by nonlinear regression using GraphPad Prism 5.0.

4.3. Free radical scavenging

The synthesized chalcone series compounds were evaluated for DPPH free radical scavenging ability. The compounds **5b**, **5e**, and **5f** showed excellent % scavenging potency, other compounds did not show significant radical scavenging potential even at high concentration (100 μg/mL) Table 1.

4.4. Structural assessment of carbonic anhydrase II

Carbonic anhydrase II (EC#: 4.2.1.1) is metal (Zn) containing protein which comprises 259 residues. The residual architecture of carbonic anhydrase II consists of 9% helices, 45% β sheets and 45% coils. The X-Ray diffraction study confirmed its resolution 1.95 Å, R-value 0.238 and unit cell dimensions like length and angles of coordinates. The computational structure assessment showed that the carbonic anhydrase II has unit cell length values (a = 103.84, b = 104.82 and c = 119.36) with angles (90°, 110.45° and 90°) for all α, β and γ dimensions respectively. Furthermore, the Ramachandran graph and values also confirms the reliability and efficacy of carbonic anhydrase II structure. The Ramachandran plots indicated that 93.8% of all residues were present in favored regions and only six poor rotamers lies in unfavored regions (Fig. 2). This selected Ramachandran graph values showed the good accuracy of phi (φ) and psi (ψ) angles among the coordinates of receptor molecules and most of residues plummeted in acceptable region.

4.5. Chemo-informatic properties and Lipinski rule (RO5) evaluation of ligands

The designed ligands were analyzed computationally to predict the best ligand on the basis of chemical and bio-molecular properties and RO5. The predicted chemo-informatic properties like Log*P*, HBD, HBA, molar volume, polar surface area (PSA) and drug likeness values of ligand molecules are mentioned in Table 1. It has been confirmed from previous research data that the standard values for molecular weight (MW) and polar surface area (PSA) are (160 to 480 g/mol) and (< 89 $Å^2$) respectively [24,]. The predicted results of compounds (5a-

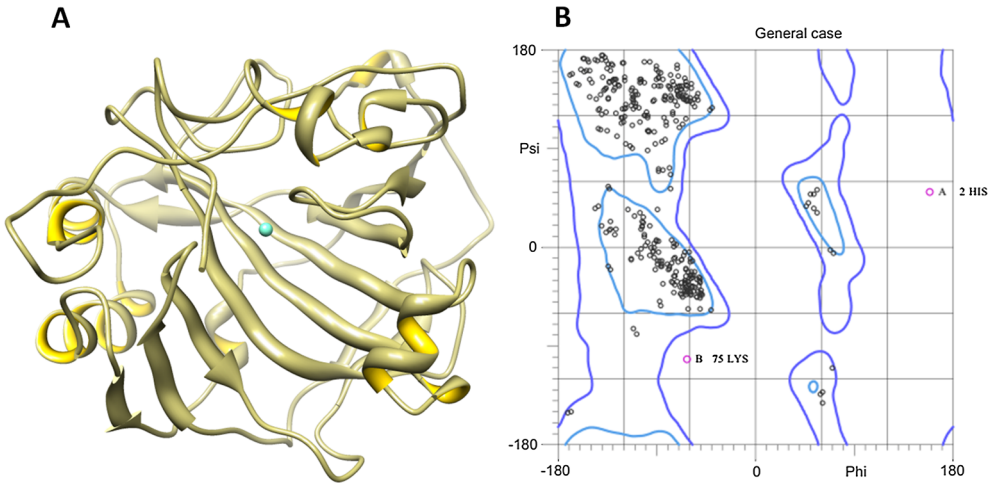

Fig. 2. (A) Crystal structure of bovine anhydrase II. (B) Ramachandran graph accessed from PDB.

5j) showed good, MW and PSA values which are comparable with standard values. RO5 also confirmed the therapeutic potential of the ligands. Hydrogen-bonding capacity has been identified as an important parameter for describing drug permeability. Research data revealed poor permeation is more likely to be observed when the HBA and HBD are exceeded then 10 and 5 respectively [25]. The chemo-informatics analysis justified that the designed compounds possess < 10 HBA and < 5 HBD. Moreover, their log*P* value were also comparable with standard value. However there are plenty of examples available for RO5 violation amongst the existing drugs [26]. The predicted chemo-informatic values of the designed ligand are mentioned in Table 1.

4.6. Molecular docking and binding energy analysis

The docked complexes of all the compounds **5a-5j** against carbonic anhydrase II were analyzed separately and evaluated on the basis of minimum energy values and ligand interactions pattern. Results showed that all compounds (**5g** and **5h**) showed good binding energy value -8.7, and -8.4 kcal/mol, respectively and exhibited in the active region of target protein (Table 2). Furthermore, **5e** showed -7.7 kcal/mol having good conformational position within the binding pocket of target protein. Prior research showed that the standard error for Autodock is testified as 2.5 kcal/mol. However, in all docking complexes the predicted energy values difference was less than standard energy value. Although, the basic nucleus of all the synthesized compounds was similar, therefore most of ligands possess good efficient energy values and have no big energy fluctuations difference. The comparative docking analysis and inhibition constant (IC_{50}) value justified that **5e** has good therapeutic potential as compared to all other compounds.

Table 2
Chemo-informatics analysis of designed chemical compounds.

Ligands	Mol. Wt (g/mol)	No. HBA	No. HBD	Mol. Log*p* (mg/L)	PSA (A^2)	Mol.Vol (cm^3)	Drug Score
5a	320.12	2	1	4.75	29.76	346.65	0.37
5b	363.17	2	1	4.87	32.57	396.20	0.10
5c	321.12	3	1	3.70	39.28	342.12	1.02
5d	350.13	3	1	4.84	37.31	378.50	0.38
5e	426.17	3	1	6.46	36.99	451.62	0.34
5f	456.18	4	1	6.55	44.53	483.47	0.30
5g	446.17	2	1	8.48	29.33	511.01	0.74
5h	549.22	7	1	4.64	82.67	593.53	0.76
5i	391.20	2	1	5.81	32.50	434.51	0.15
5j	321.12	3	1	3.70	39.19	341.95	0.85

Abbrevation: HBA = No of hydrogen bond acceptor, HBD = No of hydrogen bond donor, Log*P* = lippophilicity of partition coefficient, PSA = polar surface area.

4.7. Binding analyses of synthesized compounds against carbonic anhydrase II

The ligands-protein binding analyses showed that **5e** confined in the active binding pocket of target protein as mentioned in Fig. 3. The ligand structure showed the good conformational position closely binds near the Zn^{+2} metal. (See. Fig. 4.)

The CA II has an active site cleft (15 Å in diameter and 15 Å deep), and contains a Zn^{2+} ion that is coordinated in a tetrahedral geometry with three histidine residues (His94, His96 and His119) and a water molecule/hydroxide ion. The 5e-receptor docked complex reveals the good conformational state with hydrogen bond interactions within the receptor binding pocket. The docking result of **5e** receptor docked complex showed that three hydrogen bonds at Asp71 and Gln91 respectively. The carbonyl oxygen of **5e** interacts with Gln91 with bond distance 2.83 Å while benzyl methyl group form two hydrogen bonds against Asp71 with bond length 2.18 and 2.02 Å, respectively. Single π-

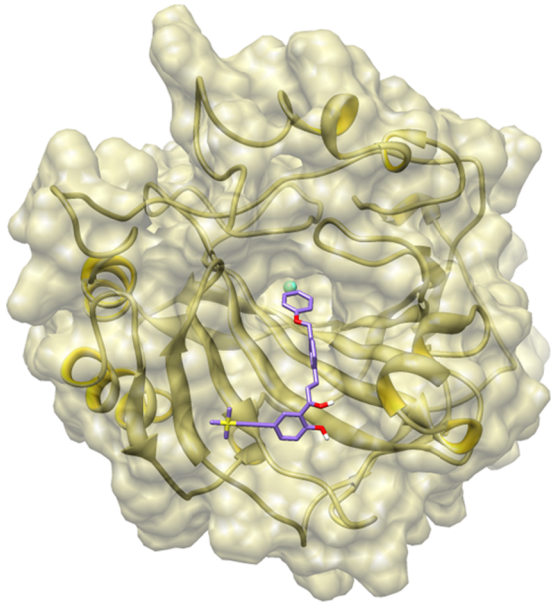

Fig. 3. Binding pocket of **5e** within the active region of carbonic anhydrase II.

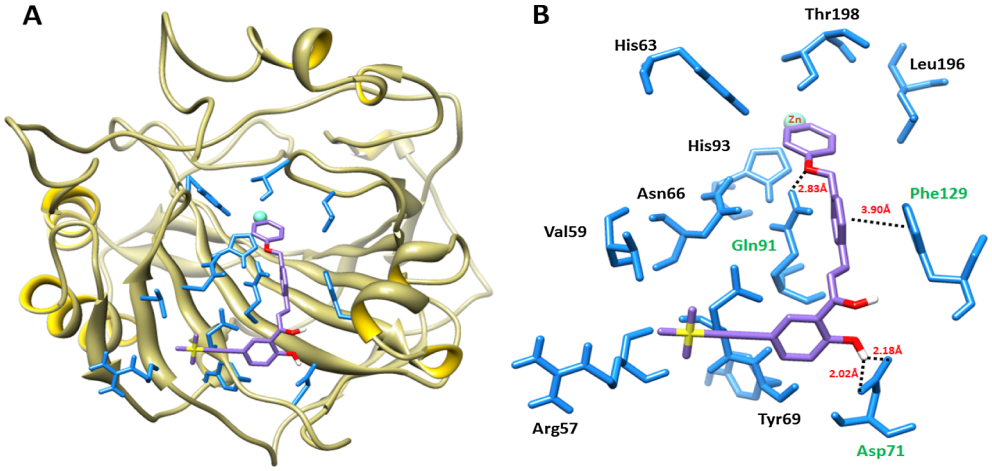

Fig. 4. Docking interaction **5e** with receptor molecule. (A) The protein structure is represented in khaki and yellow colors while the interacted residues are justified in light blue color. (B) The closer view of binding interaction. The ligand molecule is depicted in purple color while their functional groups such as oxygen and sulphur are shown in red and yellow colors, respectively. Amino acids are highlighted in black color and while light green color represent the hydrogen bonds with distance mentioned in angstrom (Å). Two hydrogen bonds were observed at Asp71 and Gln91 positions in the target protein. Zinc metal is represented in cyan color.

π stacking interaction was observed between ring structure of ligand and Phe129 having bond length 4.90 Å. Our docking results shows good correlation with published research which strengthen our work and efficacy [26]. The 2D conformations and binding pose and interactions with binding residues of all the candidate molecules are mentioned in (Figs. S1-9).

5. Conclusions

Sonogashira coupling and Claisen-Schmidt reactions were employed to obtain silyl yne containing chalcone derivatives **5a-5j**. Synthesized compounds were characterized through ^{1}H NMR and ^{13}C NMR spectroscopy. Compounds **5a-5j** were screened against carbonic anhydrase-II enzyme and antioxidant activity. The compounds displayed CA-II inhibition in micromolar range and compound **6e** having IC_{50} 0.054 ± 0.001 μM and this showed several fold time better potential than reference acetazolamide. Molecular docking studies were performed to explore the binding affinity of potent ligand **5e** in the active site of target protein and **5e** showed good binding affinity and hydrogen bonding and pi-pi stacking interactions were observed with amino acid residues. Drug score and Lipinski's rule ascertained that compound **5e** could serve as structural template and probably can be an alternate to sulfonamide drugs.

Conflict of interest

Authors declare no any conflict of interest

Appendix A. Supplementary material

Supplementary data to this article can be found online at https://doi.org/10.1016/j.bioorg.2018.11.031.

References

[1] C.T. Supuran, A. Scozzafava, A. Casini, Carbonic anhydrase inhibitors, Med. Res. Rev 23 (2003) 146–189.
[2] C.T. Supuran, A. Scozzafava, Carbonic anhydrase inhibitors and their therapeutic potential, Expert Opin. Ther. Pat. 10 (2000) 575–600.
[3] C.T. Supuran, Structure-based drug discovery of carbonic anhydrase inhibitors, J. Enzyme Inhib. Med. Chem. 27 (2012) 759–772.
[4] T.H. Maren, Carbonic anhydrase: chemistry, physiology, and inhibition, Physiol. Rev. 47 (1967) 595–781.
[5] F. Briganti, R. Pierattelli, A. Scozzafava, C.T. Supuran, Carbonic anhydrase inhibitors. Part 37. Novel classes of isozyme I and II inhibitors and their mechanism of action. Kinetic and spectroscopic investigations on native and cobalt-substituted enzymes, Eur. J. Med. Chem. 31 (1996) 1001–1010.
[6] C.T. Supuran, Carbonic anhydrases: novel therapeutic applications for inhibitors and activators, Nat. Rev. Drug Discovery 7 (2008) 168.
[7] C.T. Supuran, A. Scozzafava, Applications of carbonic anhydrase inhibitors and activators in therapy, Expert Opin. Ther. Pat. 12 (2002) 217–242.
[8] C.T. Supuran, A. Scozzafava, Carbonic anhydrase inhibitors, Curr. Medi. Chem.-Immunol., Endocrine Metabolic Agents 1 (2001) 61–97.
[9] C.T. Supuran, Carbonic anhydrase inhibitors and activators for novel therapeutic applications, Future Med. Chem. 3 (2011) 1165–1180.
[10] C.T. Supuran, F. Briganti, S. Tilli, W.R. Chegwidden, A. Scozzafava, Carbonic anhydrase inhibitors: sulfonamides as antitumor agents? Bioorg. Med. Chem. 9 (2001) 703–714.
[11] A. Innocenti, S.B.Ö. Sarıkaya, I. Gülçin, C.T. Supuran, Carbonic anhydrase inhibitors. Inhibition of mammalian isoforms I-XIV with a series of natural product polyphenols and phenolic acids, Bioorg. Med. Chem. 18 (2010) 2159–2164.
[12] A. Innocenti, D. Vullo, A. Scozzafava, C.T. Supuran, Carbonic anhydrase inhibitors: interactions of phenols with the 12 catalytically active mammalian isoforms (CA I-XIV), Bioorg. Med. Chem. Lett. 18 (2008) 1583–1587.
[13] R. Li, G.L. Kenyon, F.E. Cohen, X. Chen, B. Gong, J.N. Dominguez, E. Davidson, G. Kurzban, R.E. Miller, E.O. Nuzum, P.J. Rosenthal, In vitro antimalarial activity of chalcones and their derivatives, J. Med. Chem. 38 (1995) 5031–5037.
[14] A. Modzelewska, C. Pettit, G. Achanta, N.E. Davidson, P. Huang, S.R. Khan, Anticancer activities of novel chalcone and bis-chalcone derivatives, Bioorg. Med. Chem. 14 (2006) 3491–3495.
[15] F. Herencia, M.L. Ferrandiz, A. Ubeda, J. Domínguez, J.E. Charris, G.M. Lobo, M.J. Alcaraz, Synthesis and anti-inflammatory activity of chalcone derivatives, Bioorg. Med. Chem. Lett. 8 (1998) 1169–1174.
[16] S.N. Lopez, M.V. Castelli, S.A. Zacchino, J.N. Domínguez, G. Lobo, J. Charris-Charris, J.C. Cortés, J.C. Ribas, C. Devia, A.M. Rodríguez, R.D. Enriz, In vitro antifungal evaluation and structure–activity relationships of a new series of chalcone derivatives and synthetic analogues, with inhibitory properties against polymers of the fungal cell wall, Bioorg. Med. Chem. 9 (2001) 1999–2013.
[17] H.H. Ko, L.T. Tsao, K.L. Yu, C.T. Liu, J.P. Wang, C.N. Lin, Structure–activity relationship studies on chalcone derivatives: the potent inhibition of chemical mediators release, Bioorg. Med. Chem. 11 (2003) 105–111.
[18] N. K Sahu, S. S Balbhadra, J. Choudhary, D. V Kohli, Exploring pharmacological significance of chalcone scaffold: a review, Curr. Med. Chem. 19 (2012,) 209–225.
[19] P. Singh, A. Anand, V. Kumar, Recent developments in biological activities of chalcones: a mini review, Eur. J. Med. Chem. 85 (2014) 758–777.
[20] S Nasir Abbas Bukhari, M. Jasamai, I. Jantan, Synthesis and biological evaluation of chalcone derivatives (mini review). Mini reviews in medicinal, Chemistry 12 (2012) 1394–1403.
[21] A. Saeed, M. al-Rashida, M. Hamayoun, A. Mumtaz, J. Iqbal, Carbonic anhydrase inhibition by 1-aroyl-3-(4-aminosulfonylphenyl) thioureas, J. Enzyme Inhib. Med. Chem. 29 (6) (2014) 901–905.
[22] Q. Abbas, Z. Ashraf, M. Hassan, H. Nadeem, M. Latif, S. Afzal, S.Y. Seo, Development of highly potent melanogenesis inhibitor by in vitro, in vivo and computational studies, Drug Design, Development Therapy 11 (2017) 2029.
[23] M. Hassan, Q. Abbas, Z. Ashraf, A.A. Moustafa, S.Y. Seo, Pharmacoinformatics exploration of polyphenol oxidases leading to novel inhibitors by virtual screening and molecular dynamic simulation study, Comput. Biol. Chem. 68 (2017) 131–142.
[24] Z. Iqbal, M. Hassan, J. Munir, I.M. Farah, R. Shakoori, A.R. Shakoori, Identification of novel dihydrofolate reductase inhibitor as potential antimalarial drug: in silico studies, Pakistan J. Zool. 46 (5) (2014).
[25] Q. Abbas, R. Hussain, A.A. Moustafa, S.Y. Seo, Computational analysis of histidine mutations on the structure stability of human tyrosinases leading to albinism insurgence, Molecular BioSystems (2017).
[26] Q. Abbas, M. Hassan, H. Raza, S.J. Kim, K.W. Chung, G.H. Kim, S.Y. Seo, In vitro, in vivo and in silico anti-hyperglycemic inhibition by sinigrin, Asian Pacific J. Tropical Med. 10 (4) (2017) 372–379.